ACCSCIENCE PUBLISHING

International Journal of Bioprinting

RESEARCH ARTICLE

Development of an *in situ* 3D bioprinting and laser-assisted wound care model: From leech regeneration to space medicine applications

Supplementary File

S1. In situ bioprinting design

S1.1. Picture acquisition of the printing bed

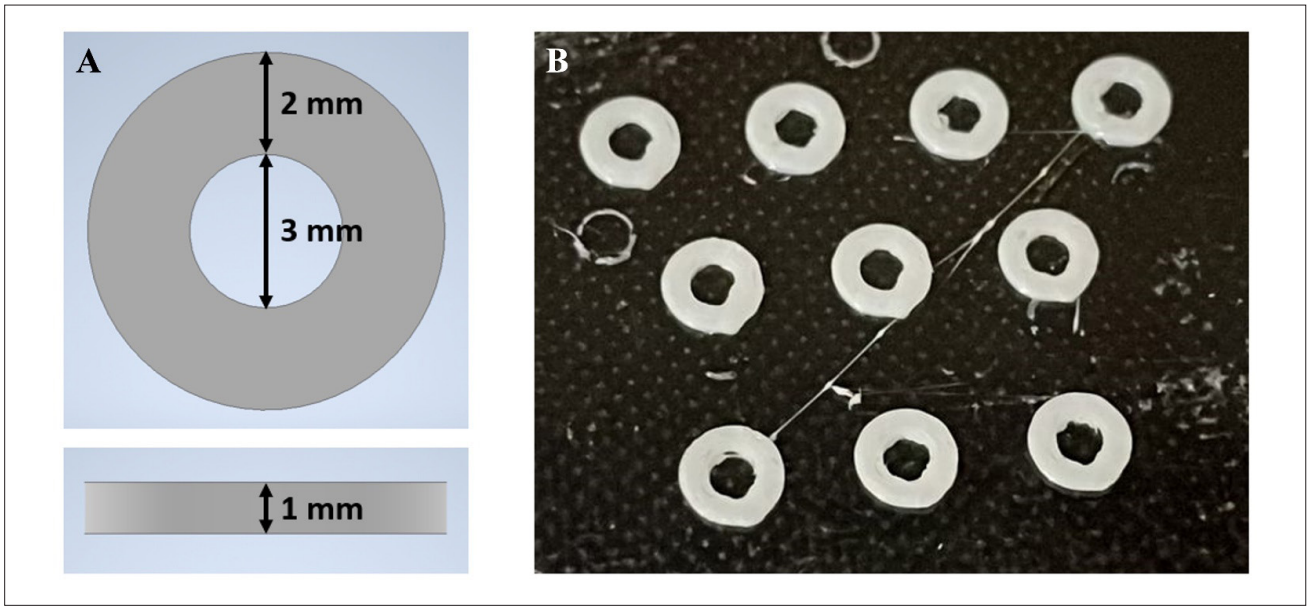

Figure S1. Printing of circular-shaped objects to highlight the wound during the procedure. (A) Computer-aided design model on Autodesk Inventor. (B) Printing results.

S1.2. Image segmentation

The image segmentation procedure can be divided into the following five phases.

(i) Image reading: Images of the printing plate and the object on which to print were imported into MATLAB (Figure S3A).

(ii) Image binarization: A complement image was generated, and the image was binarized by choosing an appropriate threshold that allowed the identification of all necessary structures (i.e., the printing plate and the object of interest) (Figure S3B).

(iii) Contour pixel selection: The boundary pixels of all features in the binarized image were extracted. Then, the contour pixels of the printing plate and the objects of interest were selected (Figure S3C).

(iv) Transformation of contour pixels in coordinates: The fourth step aims to extract the correct motion

coordinates from each image so that the 3D printer can bioprint on the object of interest. To this end, the contour pixels selected in Step 3 were converted to coordinates in the correct reference system, accounting for the actual dimensions of the printing plate (Figure S3D).

(v) Coordinate saving: The last step was to save the extracted coordinates of the objects of interest in an XLSX file. XLSX format can be easily read by Autodesk Inventor for computer-aided design model development.

To ensure high usability, an application based on the above-described steps was developed using MATLAB's App Designer. In the first window (Figure S3E), the "Select the picture" button allows the user to choose, import, and view the desired picture from a folder. Using a slicer, one can select a threshold for binarization and view the resulting image in real time. Using the "Extract the contours" button, a second window (Figure S3F) allows viewing all extracted contours and selects only the contour pixels of interest, which are converted to coordinates and shown in a plot. If the contour pixels are not exact, the user can return to the previous window through the "Change the threshold" button and modify the binarization threshold. If the contours appear correctly set, they can be saved and exported as an XLSX file using the "Generate XLSX file" button.

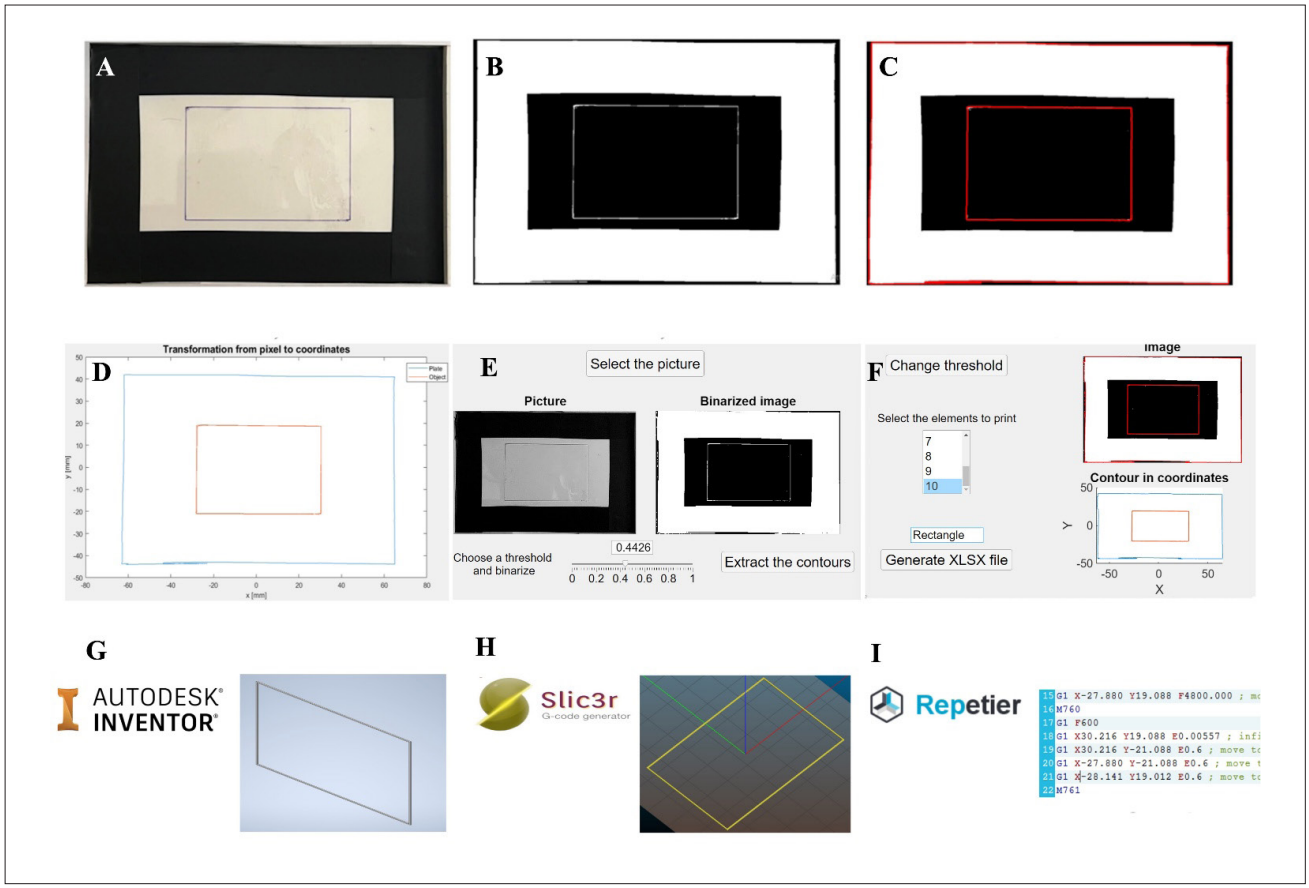

Figure S2. Image processing: From segmentation to G-code generation. (A) Image reading. (B) Image binarization. (C) Contour pixel selection. (D) Transformation of contour pixels into coordinates. Application created using App Designer in MATLAB. (E) First window to select, import, and binarize the image. (F) Second window to choose the contour pixels and generate the XLSX file. (G) Uploading the XLSX file to the Inventor software and extracting the computer-aided design (CAD) model. (H) Importing the CAD model and slicing process using Slic3r software. (I) Generation of the G-code ready for *in-situ* bioprinting using the Repetier software.

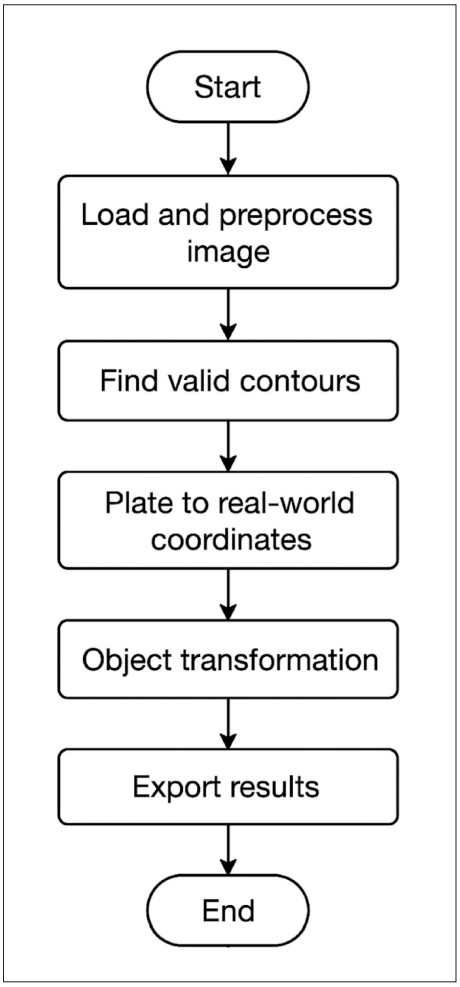

Figure S3. MATLAB pseudocode summary diagram.

S1.3. Software validation

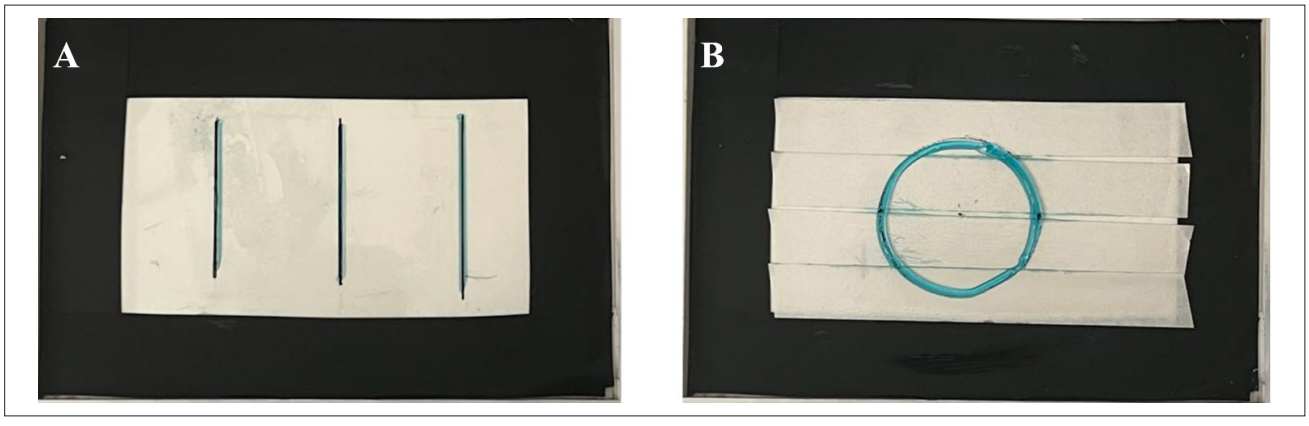

Figure S4. Monolayer validation. (A) Three separate straight lines. (B) Circle.

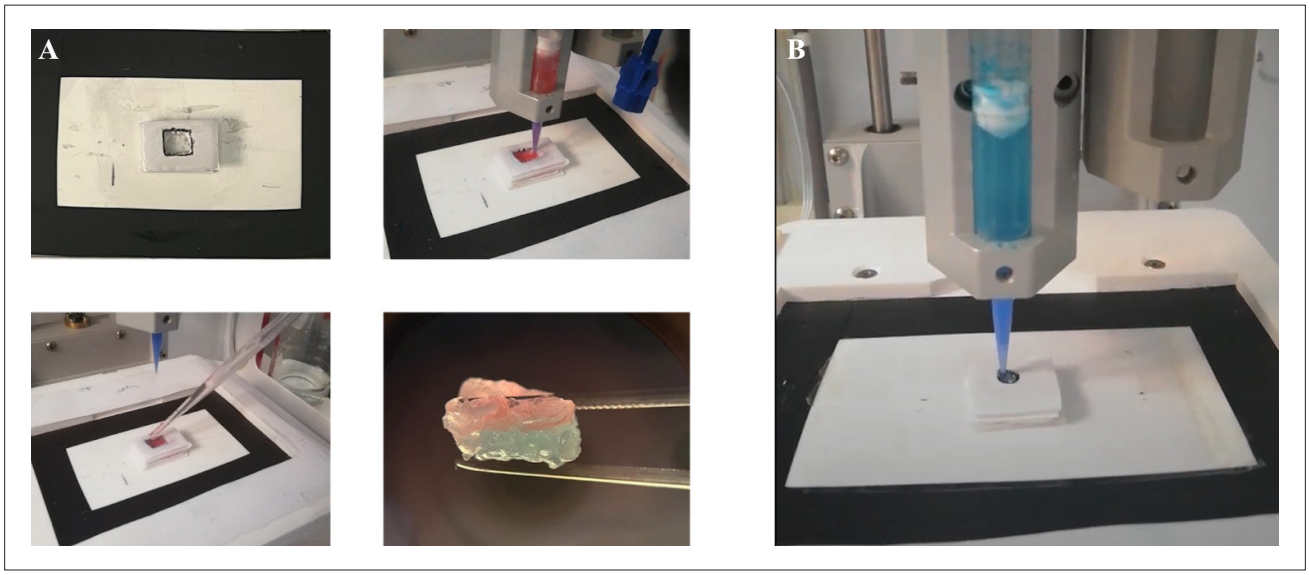

Figure S5. Multilayer validation. (A) Printing plate with the support. (B) Printing within the support. (C) Cross-linking with calcium chloride. (D) Printing result. (E) Validation with a cylindrical hole.

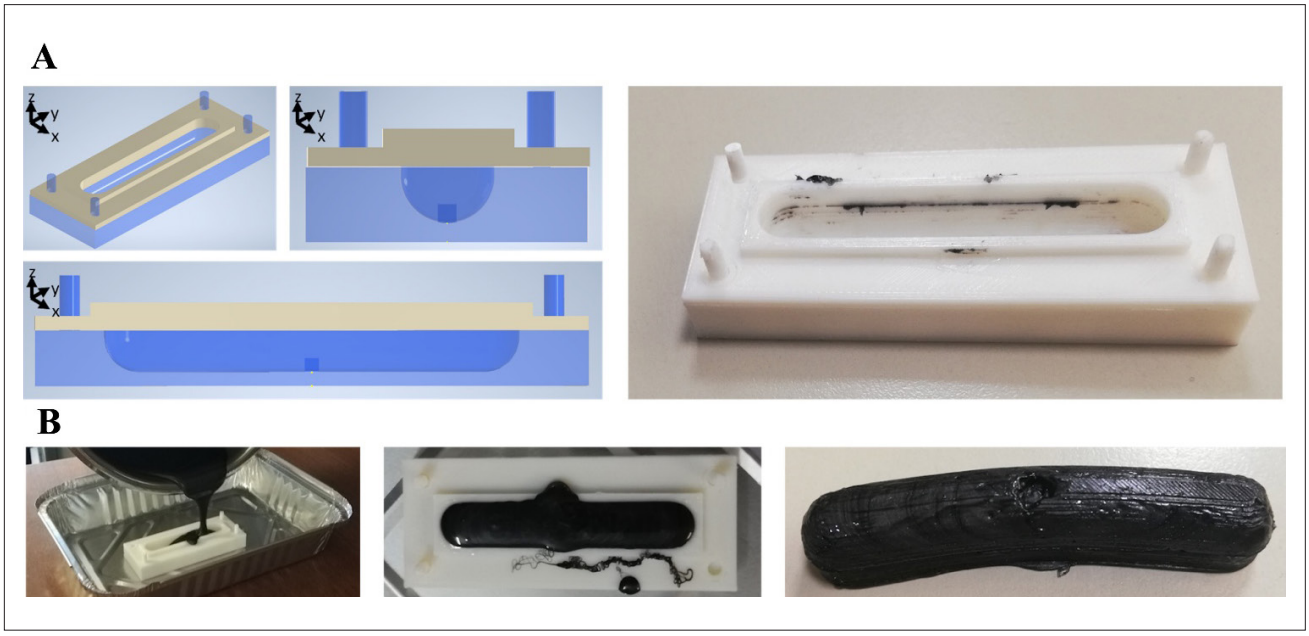

Figure S6. Phantom fabrication. (A) Computer-aided design model of the mold. (B) 3D-printed mold. (C) The ballistic gelatin is poured into the mold. (D) The gel is left to dry. (E) Phantom results.

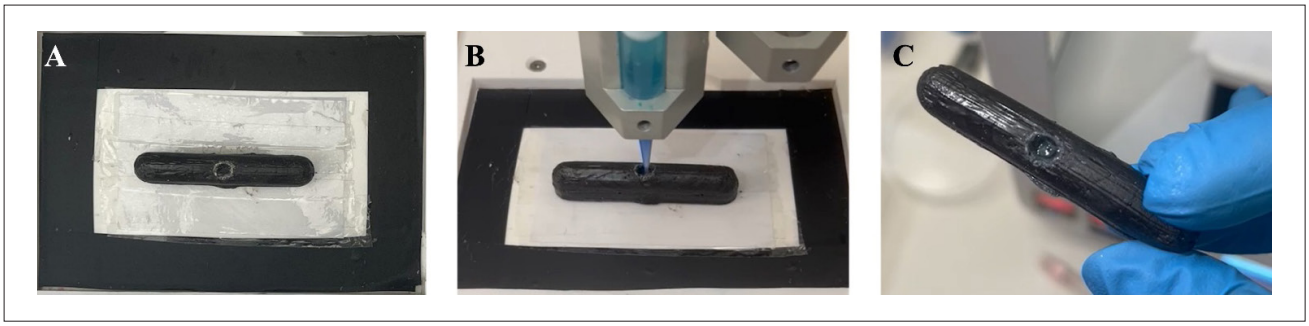

Figure S7. 3D printing on the leech phantom. (A) Phantom placement on the printing plate. (B) 3D printing within the phantom. (C) 3D printing result.

S1.4. *In situ* bioprinting in the leech wound model

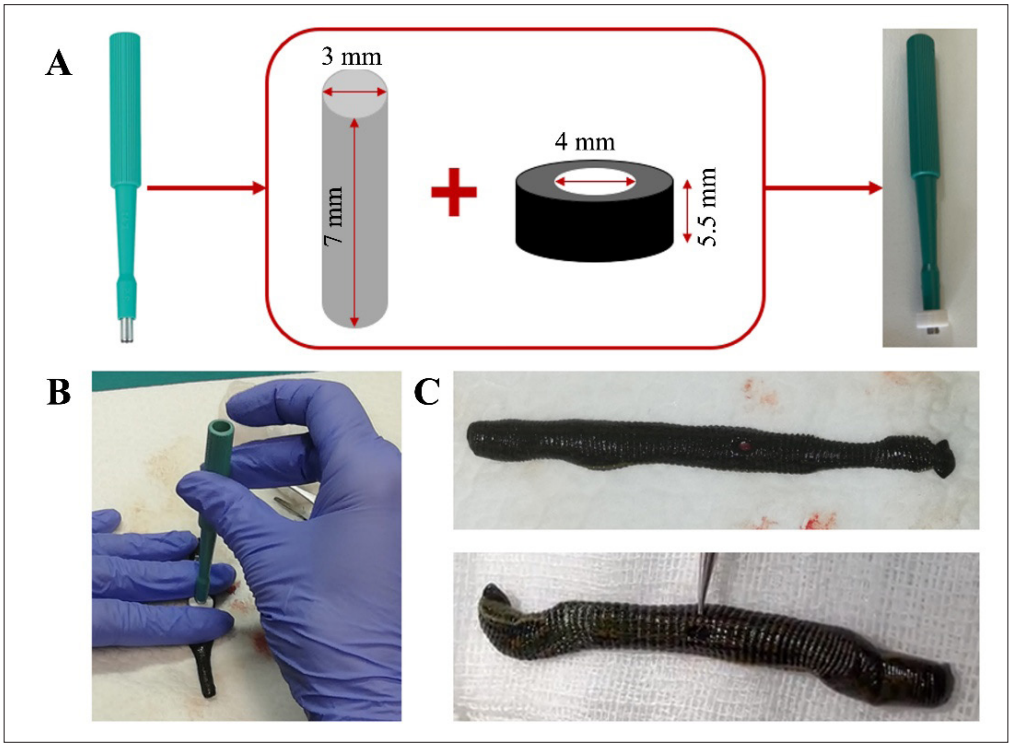

Figure S8. Preparation of the leech wound model. (A) Design of an adapter for the surgical punch. (B) Biopsy of the leech. (C) Examples of two wounded leeches.

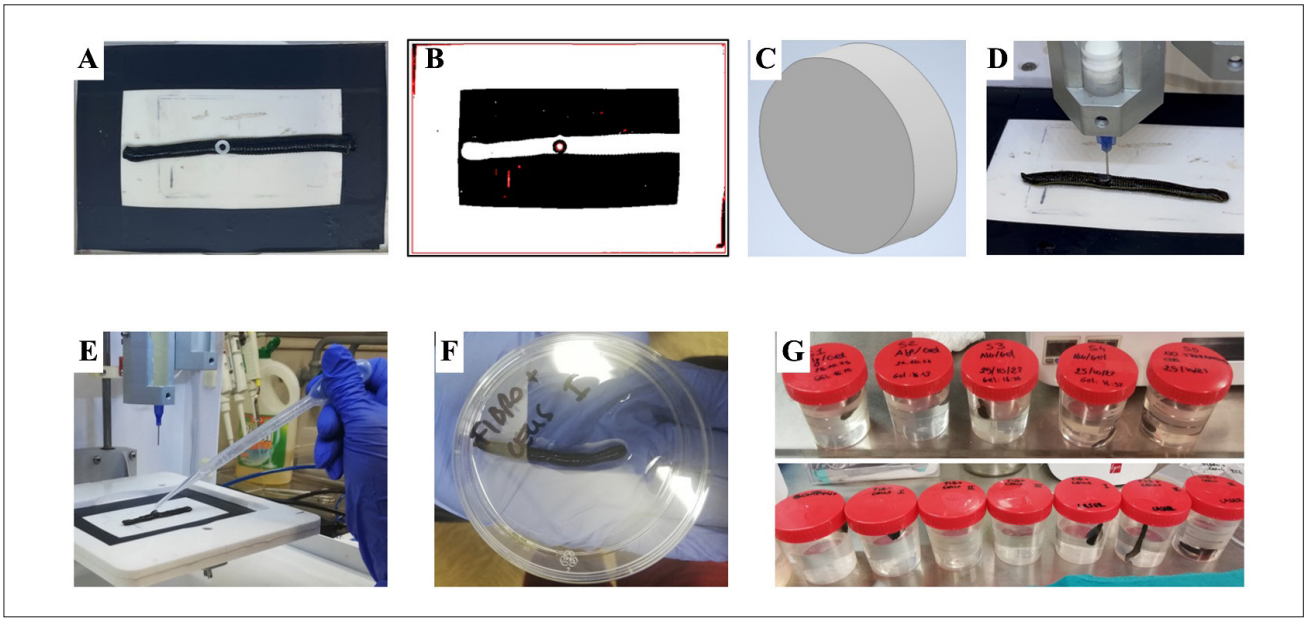

Figure S9. *In situ* 3D bioprinting procedure on a leech animal model. (A) Picture of the wounded leech on the printing plate. (B) Contour pixels obtained through the developed MATLAB code. (C) Computer-aided design model of the wound. (D) 3D bioprinting on the wounded leech. (E) $CaCl_2$ application to cross-link. (F) Leech in a phosphate-buffered saline to stabilize the wound. (G) Isolated leeches after printing.

S2. Rheological and mechanical properties of the biomaterial inks

Rheological and mechanical characterization is essential for reproducibility and printability assessment. For this reason, we chose to use two hydrogels whose rheological behavior has been extensively studied. Specifically, in the study by Cavallo *et al.*,[1] the rheological and mechanical behavior of a fibrinogen–alginate hydrogel was studied. The rheological properties were evaluated through rotational (shear rate sweep) and oscillatory (amplitude and frequency sweeps) tests performed at 25°C and 37°C (room temperature and physiological temperature, respectively). At both testing temperatures, the formulation showed decreasing viscosity with increasing shear rate; therefore, the fibrinogen–alginate hydrogel is a non-Newtonian fluid with shear-thinning behavior (Figure S10A). Furthermore, the mechanical properties of the fibrinogen–alginate hydrogel were also studied using three bioprinted samples (diameter of 8 mm and height of 5 mm) and a uniaxial testing machine with a 10 N load cell at 1 mm/min with a maximum displacement of 60%. The compressive modulus of cross-linked samples of fibrinogen-based biomaterial ink was calculated considering the linear slope of the stress–strain curve (10% of strain) before the hydrogel yield point. A compressive modulus of 36.5 ± 9.7 kPa was calculated (Figure S10B). Additionally, specifically for the commercial CELLINK Fibrin hydrogel, the manufacturer reports a viscosity of 2.6–7.5 kPa·s at a shear rate of 0.01/s, and 1.0–1.9 Pa·s at 200/s. These measurements were obtained using an HR-10 TA Instruments Rheometer with 20 mm plate–plate geometry, employing a steady-state rotational flow sweep at 25°C over a shear rate range from 0.001/s to 200/s.

Regarding the alginate- and gelatin-based (SA/GEL) hydrogel, its rheological properties were extensively studied by Di Gravina *et al.*[2] In shear rate ramp tests, the SA/GEL formulation exhibited shear-thinning behavior, with viscosity decreasing as shear rate increased. The degree of shear-thinning, expressed as the power-law index (n), was quantified by fitting viscosity–shear rate data to the Power law model. The SA/GEL hydrogel showed a value of 0.256, with a good linear fit (R^2 = 0.99), indicating pronounced shear-thinning attributes (Figure S10C). Furthermore, Dey *et al.*[3] conducted compression tests ranging from 0% to 20% strain on various SA/GEL hydrogel formulations under oscillatory time conditions, using a strain amplitude of 1% and a frequency of 1 Hz. The results are presented in Figure S10D.

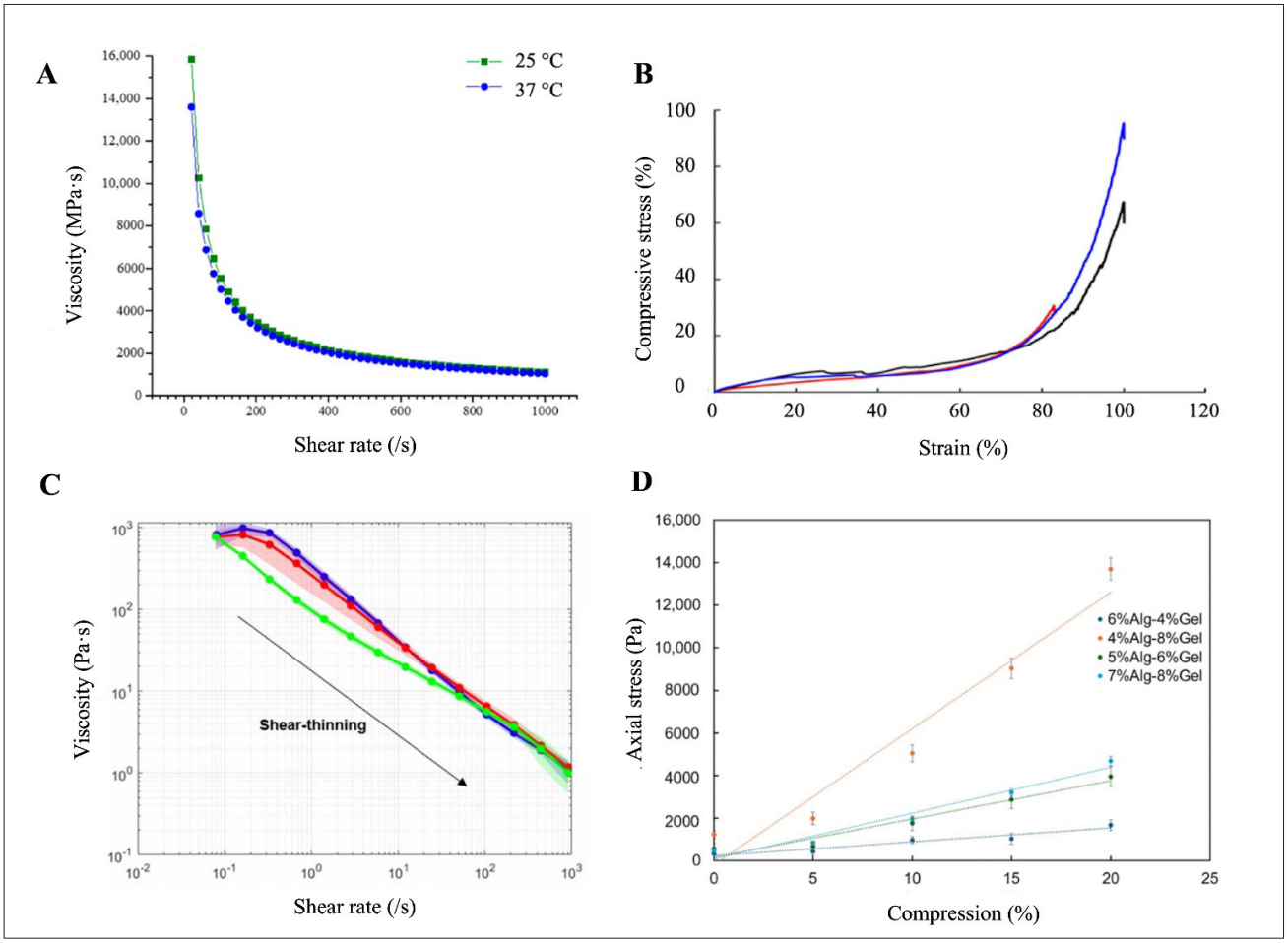

Figure S10. Characterization of biomaterial inks. (A) Rheological and (B) mechanical characterization of the fibrinogen-based biomaterial ink. Reprinted from Cavallo *et al.*[1] (C) Rheological (reprinted from Di Gravina *et al.*[2] Copyright © 2023 The Author[s]) and (D) mechanical characterization of the sodium alginate-gelatin biomaterial ink (reprinted from Dey *et al.*[3]).

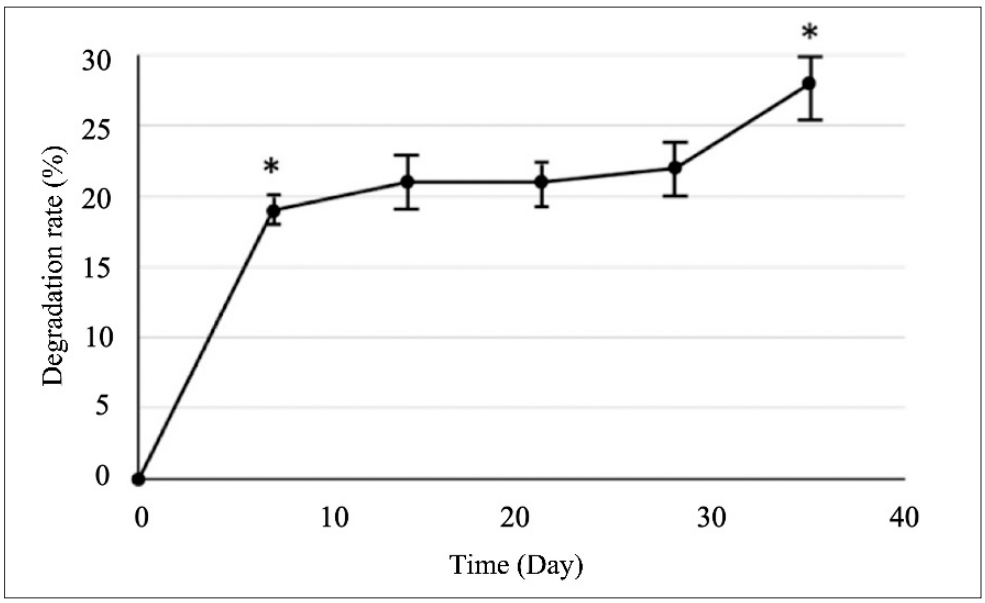

Figure S11. Degradation rate of a fibrinogen- and alginate-based biomaterial ink. Reprinted from Cavallo *et al.*[1]

References

1. Cavallo A, Al Kayal T, Mero A, *et al*. Fibrinogen-based bioink for application in skin equivalent 3D bioprinting. *J Funct Biomater*. 2023;14(9):459.
doi: 10.3390/jfb14090459

2. Di Gravina GM, Bari E, Croce S, *et al*. Design and development of a hepatic lyo-dECM powder as a biomimetic component for 3D-printable hybrid hydrogels. *Biomedical Materials*. 2023;19(1):015005.
doi: 10.1088/1748-605X/ad0ee2

3. Dey MK, Devireddy RV. Rheological characterization and printability of sodium alginate–gelatin hydrogel for 3D cultures and bioprinting. *Biomimetics*. 2025; 10(1):28.
doi: 10.3390/biomimetics10010028